

Rapid assessment of petroleum-contaminated soils with infrared spectroscopy



Wartini Ng ^{*}, Brendan P. Malone, Budiman Minasny

Centre for Carbon, Food & Water, Faculty of Agriculture & Environment, University of Sydney, NSW 2006, Australia

ARTICLE INFO

Article history:

Received 15 April 2016

Received in revised form 24 October 2016

Accepted 22 November 2016

Available online 14 December 2016

Keywords:

Soil contamination

Soil sensing

Petroleum hydrocarbon

Spectroscopy

Mid infrared

ABSTRACT

Soil sensing using infrared spectroscopy has been proposed as an alternative to conventional soil analysis to detect soil contamination. This study evaluated the use of field portable and laboratory benchtop infrared spectrometers in both the near infrared (NIR) and mid infrared (MIR) region for rapid, non-destructive assessment of petroleum contaminated soils. A laboratory study of soils spiked with petroleum products showed that several factors can affect the infrared absorbance. These include soil texture, organic matter content, and the types and concentrations of contaminants. Despite these factors, infrared regions that are affected by hydrocarbon contamination can be readily found in 2990–2810 cm⁻¹ in the MIR range, and 2300–2340 nm in the NIR range. Using continuum-removed spectra, the effects of soil and contaminant factors on the absorbance peaks were isolated. This study also created statistical models to predict total recoverable petroleum hydrocarbons concentration in soils by utilizing the absorption features found in the mid-infrared region spectra. Subsequently, three different approaches were tested for the prediction of Total Recoverable Hydrocarbon (TRH) concentration on 72 field contaminated samples: (i) linear regression using only 1 infrared region, (ii) multiple linear regression (MLR) using 4 regions in the MIR, and (iii) partial least square regression (PLSR) which use the whole spectra. The model created using MLR approach for portable MIR spectrometer outperformed the benchtop MIR spectrometer with a coefficient of determination (R^2) of 0.71 and 0.53 respectively. While PLSR model for portable spectrometer show a better prediction for TRH prediction ($R^2 = 0.75$), the MLR can also achieve a similar performance ($R^2 = 0.71$) by using only 4 regions in the MIR spectra as predictors.

© 2016 Elsevier B.V. All rights reserved.

1. Introduction

Petroleum contamination in soil has been recognized as a globally significant issue. It poses health risks to humans and wildlife in the surrounding environment. Petroleum contamination in soil is mostly due to the process of production, storage and distribution of the petroleum products. If the contamination levels exceed regulatory standards, clean-up measures need to be considered. Health Screening Levels (HSL) and Ecological Screening Levels (ESL) for petroleum products have been developed to address the risks associated with petroleum contamination on human health and ecosystems respectively (NEPC, 2011a). With millions of potentially contaminated soil sites in the world (CRCCARE, 2015), there needs to be rapid and efficient on-site assessment technologies that are able to analyse the concentration of the petroleum hydrocarbons.

Conventional methods to analyse soil contamination in the laboratory is not only time consuming, but also expensive (Viscarra Rossel et al., 2011; Okparama and Mouazen, 2013a; Chakraborty et al., 2015; Horta

et al., 2015). The most commonly used analytical method for determining petroleum hydrocarbons in soil is extraction using chemical solvents, where the extracts are subjected to a gas chromatography (GC) system equipped with a flame ionization detector (FID) following US EPA method 8015B (Sadler and Connell, 2003). The cost to analyse a sample using this conventional method starts from \$100 per sample, and requires a significant investment of time and technical skills (Chakraborty et al., 2015). Furthermore, it is often found for repeated measurements that there can be considerable variation within lab, and particularly inter-lab variability for the same phenomena (Schwartz et al., 2012; Chakraborty et al., 2015).

To successfully distinguish petroleum contamination in soil, sensing with optical and radiometric sensors is preferred (Viscarra Rossel et al., 2010). Optical and radiometric sensors utilize electromagnetic energy to characterize soil, particularly those in the near-infrared and mid-infrared region. Infrared (IR) spectroscopy could be a viable alternative in soil sensing to provide measurements in a timely and cost-effective manner (Chakraborty et al., 2015; Horta et al., 2015). A number of studies have investigated the feasibility of infrared technologies for the rapid assessment of Total Petroleum Hydrocarbons (TPH) concentration in soil. Some of these include studies conducted by Forrester et al.

* Corresponding author.

E-mail address: wartini.ng@sydney.edu.au (W. Ng).

(2013), Okparanma and Mouazen (2013a), Schwartz et al. (2012), and Horta et al. (2015). Although the infrared technologies had been used since the 1960s, it has gained much popularity in the last 20 years. This trend has coincided with the development of portable infrared instruments, chemometrics and statistical methods (Viscarra Rossel et al., 2011; Okparanma and Mouazen, 2013a). Sample scanning with infrared spectrometers only takes a matter of seconds, requires no chemicals, and facilitates the possibility to infer a number of soil properties simultaneously (Okparanma and Mouazen, 2013b; Horta et al., 2015).

TPH is a term used to describe the quantity of petroleum-based hydrocarbon products in the environment, such as crude oil and its derivatives. Currently in Australia, hydrocarbon contamination is reported as Total Recoverable Hydrocarbons (TRH) instead of TPH. This change is adopted to provide reliable site contamination assessments because TRH reflects what can be extracted, while TPH indicates what is actually present in the soil (NEPC, 2011b). Different soil components create unique interactions with the hydrocarbons, preventing them to be extracted completely. The strength of hydrocarbon sorption in the soil is affected by the nature of the hydrocarbon, organic matter content and soil minerals (Sadler and Connell, 2003).

The objectives of this study were to: 1) determine which spectrum range could be used to quantitatively assess petroleum hydrocarbons using the laboratory mid-infrared (MIR), portable MIR (pMIR), and portable Visible-NIR (pNIR) spectrometers, 2) observe the effect of soil texture and organic matter on the peak intensities of spectra, 3) observe the effect of various types and concentrations of petroleum hydrocarbons on the spectra, 4) monitor the degradation of petroleum hydrocarbons through time, 5) construct theoretical models to quantify the amount of petroleum hydrocarbon contamination based on significant NIR and/or MIR spectra bands, and validate them with field contaminated samples.

2. Materials and methods

This study comprised of two experiments. The first experiment examined the effect of soil type, organic matter content, and concentration of two types of petroleum on the near- and mid-infrared reflectance spectra. The study was done under laboratory conditions, where a known concentration of hydrocarbon material was added to the soil. In the second part of the experiment, we used field contaminated soils which had been contaminated with petroleum, with the aim to create and validate models which can predict TRH concentration from infrared spectra data.

2.1. Laboratory contaminated soils

The soil samples used in this part of experiment were obtained from University of Sydney Lansdowne Farm ($34^{\circ}02'S$, $150^{\circ}66'E$) in NSW, Australia. This study was conducted on a total of 126 samples with factors and levels as follows: 2 soil texture types (clayey, sandy), 3 levels of organic matter addition (0%, 1%, 3%), 2 types of organic contaminants (diesel, motor oil) at 3 concentration levels (0 ppm, 5000 ppm, 10,000 ppm, 30,000 ppm) in replicates of three.

The clayey soil (Red Chromosols according to Australian Soil Classification System (ASC) or Alisols according to World Reference Base for Soil Resources (WRB)) contained 48% sand (20–2000 μm), 13% silt (2–20 μm), and 39% clay (<2 μm) by mass, with clay mineralogy dominated by kaolinite. The sandy soil (Orthic Tenosols (ASC) or Arenosols (WRB)) contained 88% sand, 4% silt, and 9% clay by weight, dominated by SiO_2 and kaolinite.

Soil samples were first air-dried at 40°C for 3 days, then ground and sieved to pass through a 2-mm sieve. Moisture content of the samples was determined by drying the soil at 105°C for 16 h in the oven. From the moisture content analysis, the dry weight of the soil is determined. An equivalent of 25 g of oven-dry soil of each soil type was then placed into the designated petri dishes.

Soil organic carbon content was determined using Vario MAX CNS Analyzer (Elementar, Langenselbold, Germany). The clayey soil and the sandy soil contained 0.60% and 0.15% organic carbon by mass, respectively. Organic matter in the form of organic compost (PMR0320, RichGro, Jandakot, WA, Australia) was added onto the samples until the increase of 1, and 3% in C was achieved.

These soil samples were then wetted to 75% field capacity to maintain their moisture and incubated for 3 weeks before being spiked with the petroleum hydrocarbons. Aliquots of 0, 0.15, 0.30 and 0.60 mL of motor oil and diesel fuel were mixed with 10 mL of cyclohexane (Sigma Aldrich, Castle Hill, NSW, Australia) to give soils with TPH concentration ranging from 0, 5000, 10,000 to 30,000 ppm. Cyclohexane was used as a solvent to ensure even distribution of petroleum hydrocarbons throughout the samples (Forrester et al., 2010). The petri dishes were left open to allow spiked samples dry overnight to remove traces of cyclohexane. The motor oil used was Valvoline 2-stroke engine oil. The experiment was carried out at a room temperature of $\sim 25^{\circ}\text{C}$ for 11 weeks after soil was spiked. Measurement using infrared spectrometers was conducted every 2–3 weeks. After each measurement, the samples were re-wetted and covered to observe the effect of time on the petroleum degradation.

2.2. Spectral measurements

The reflectance spectra of each sample were obtained using a benchtop MIR, a portable MIR and a portable NIR spectrometer. To remove the effect of moisture, the samples were left open to dry overnight at laboratory temperature of $\sim 25^{\circ}\text{C}$ prior to measurement. The samples were then mixed thoroughly and tamped flat. The spectra were obtained as an average of 2 replicate scans in a different spot to ensure the heterogeneity of samples was captured.

2.2.1. MIR spectral acquisition

The MIR spectrum covers the range of $4000\text{--}400\text{ cm}^{-1}$ (2500–25,000 nm). Resulting spectra from the absorbed and transmitted infrared radiation by the sample correspond to the fundamental molecular vibration of the sample. Laboratory benchtop MIR spectra were obtained from FTIR TENSOR 37 (Bruker Optics, Ettlingen, Germany) equipped with HTX-XT micro-plate reader automated sampler, with a spectral range acquisition between 3996 and 599 cm^{-1} at 4 cm^{-1} resolution and $\sim 2\text{ cm}^{-1}$ sampling interval. Potassium bromide (KBr) was used as a standard in this MIR spectrometer. The portable MIR spectra were obtained from the RemScan (Ziltek Pty Ltd, Adelaide, Australia) or equivalent to Agilent 4100 ExoScan (Agilent Technologies, Santa Clara, CA, United States) which collected reflectance between 6000 cm^{-1} and 650 cm^{-1} at 8 cm^{-1} resolution and $\sim 2\text{ cm}^{-1}$ sampling interval. This instrument was calibrated with the standard background and a reference cap provided by the manufacturer.

2.2.2. NIR spectral acquisition

The NIR region covers the range between 780 and 2500 nm. Spectra in this region correspond to combinations and overtones of the fundamental molecular vibration bands (2000–2500 nm) found in the mid

Table 1
Band assignments observed in the MIR spectra.

Wavenumber (cm^{-1})	Band assignments
1630–1580 ^a	Aromatic C=C conjugated with C=O
1930–1840 ^a	Aromatic CH, C=O acid anhydrides
2060–1930 ^a	Cumulative C=C bonds, aromatic CH
2990–2810 ^a (2930–2850 ^b , 3000–2600 ^c)	Aliphatic —CH ₂ or —CH ₃
3630–3620 ^b	Clay minerals (smectite and illite)
3690–3620 ^b	Clay minerals (kaolinite)

^a Band assignments after Hobley et al. (2014).

^b Band assignments after Soriano-Disla et al. (2014).

^c Band assignments after Forrester et al. (2013).

infrared region. The intensity of the derived absorption decreases when the overtone increases. Band intensities observed in NIR are usually much weaker and broader than the corresponding bands found in the MIR.

The portable Vis-NIR spectra were obtained from AgriSpec Vis-NIR (Analytical Spectral Devices, Boulder, CO, United States) with a spectral range of 350 to 2500 nm with 1 nm sampling interval and resolution of 3 nm (at 700 nm) to 10 nm (at 1400 nm). Soils were illuminated with a 4.5 W built-in halogen light source, and the reflected light was transmitted to the spectrometer. A Spectralon (Labsphere Inc., North Sutton, NH, USA) white standard was used for instrument calibration, and measured every 10 scans for baseline correction. Although NIR spectra were difficult to interpret, attempts were made to extract indicative bands for hydrocarbons by chemometric methods.

2.2.3. Spectral data analysis

All collected spectra were converted from reflectance (R) to absorbance by $\log(1/R)$, smoothed using the Savitzky-Golay (SG) algorithm with a window size of 21 and polynomial of order 2, and followed by Standard Normal Variate (SNV) transformations. SG algorithm is used to remove instrument noise within the spectra by smoothing the data using the polynomial regression, while SNV is used to normalize the spectra, scaling it to zero mean and unit standard deviation (Rinnan et al., 2009).

To address the effect of organic matter, spectra of soil without organic matter addition was subtracted from the spectra of soil with added organic matter. In the NIR spectra, where changes in the absorbance peak were hard to be observed, the first-derivative of the spectra was used to find the indicative wavelengths.

To quantify the TRH concentration, a continuum removal technique was used to enhance absorption features in the spectra (Clark and Roush, 1984). A continuum-curve was created by fitting a convex hull

over the top of the local maxima of the absorbance spectra. The absorbance spectra were then subtracted by the continuum-curve, creating new continuum-removed baseline spectra. From the new continuum-removed spectra, absorption features for certain peaks were isolated and used for comparison (Clark, 1999). The effect of different test parameters was compared based on the position, band width, band depth and areas between continuum-curve and the continuum-removed spectra. All computations were performed in the open source software R (R Core Team, 2016).

2.3. Field contaminated samples for model validation

To be able to predict petroleum contamination on the field contaminated samples, attempts to create calibration statistical models were made from both MIR and NIR spectra analysis of laboratory contaminated samples. The models would be based on integrated areas under various peaks that were affected by TRH concentration and other functional groups which were identified by Hobley et al. (2014).

A total of 72 soil samples obtained from a soil recycling facility in New South Wales, Australia were used to test the validity of the statistical models. These samples were scanned in the same manner as the laboratory contaminated samples. All samples were collected from the same undisclosed locations taken at different times. These samples had been contaminated with petroleum and undergone treatment by the addition of organic matter in the remediation processes. Conventional laboratory analysis of the samples were obtained from the National Measurement Institute (North Ryde, NSW, Australia) which analysed the Total Recoverable Hydrocarbons (TRH) that represented amounts of extracted petroleum hydrocarbons by selected solvents.

The samples were analysed in a certified laboratory following USEPA SW846 8270D method. Total recoverable hydrocarbons in the C₆–C₉ fraction, including Benzene, Toluene, Ethylbenzene and Xylene (BTEX)

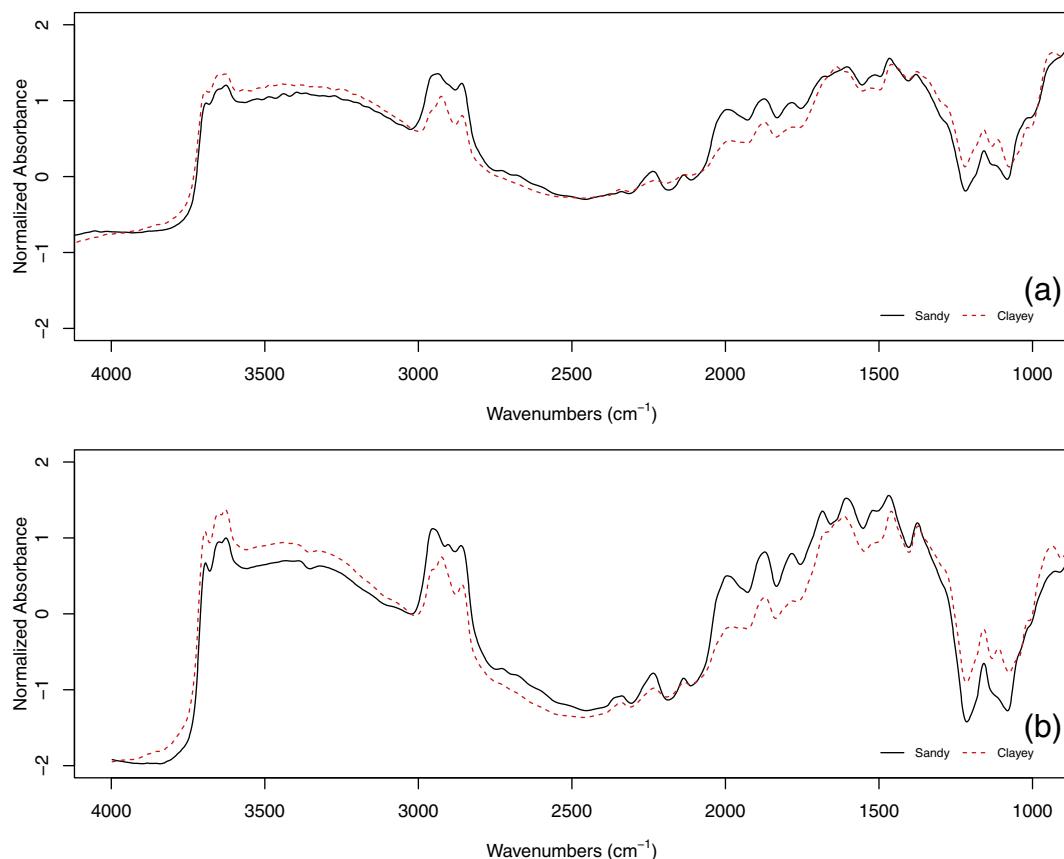


Fig. 1. Absorbance spectra of different types of soil samples spiked with 30,000 ppm of motor-oil, scanned by using (a) portable and (b) laboratory benchtop MIR spectrometer.

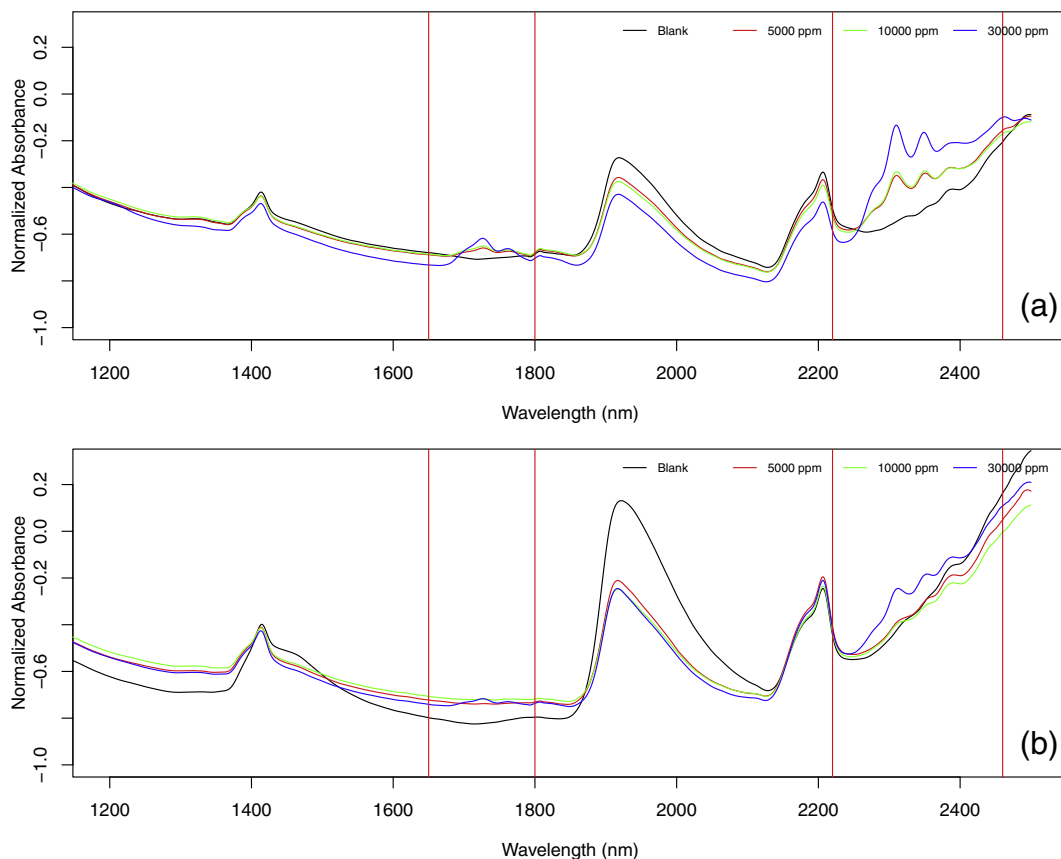


Fig. 2. NIR spectra of (a) sandy and (b) clayey soil spiked with various concentrations of diesel. Peaks on combination (2220–2460 nm) and first overtone region (1650–1800 nm) were identified to be related to the TRH concentrations.

were analysed using the Purge & Trap GC/MS method. Fractions C₁₀–C₁₆, C₁₅–C₂₈ and C₂₉–C₃₆ were first extracted using dichloromethane/acetone then analysed by Gas Chromatography and detection by flame ionization. TRH is expressed as a sum of all the fractions (C₆–C₃₆) (NEPC, 2011b). The TRH values of these samples ranged from 0 to 17,240 ppm with a median concentration of 4620 ppm.

Linear Regression (LR), Multiple Linear Regression (MLR) and Partial Least Squares Regression (PLSR) models were compared. The LR model using NIR region utilized bands between 2300 and 2340 nm, while the LR model in MIR region only utilized the bands between 2990 and 2810 cm⁻¹, which is directly correlated with the aliphatic —CH₂ groups. A stepwise linear regression approach was used in the MLR model to select significant predictors for TRH from a range of functional groups identified by Hobley et al. (2014). The PLSR models were derived from re-sampled spectra (averaging the spectra every 10th wavelength) based on the full spectra to reduce data dimension. A leave-one-out cross-validation approach was used to select the number of components for the PLSR.

The accuracy of the models was assessed with the R² (coefficient of determination), and RMSE (root mean squared error). For model performance and selection, the leave-one-out cross validation (cv) method, which repeatedly single out an observation as a validation set and use the remaining observations as the training set, was used (Hastie et al., 2009). In addition, another model selection criteria which considers the complexity of models (number of parameters) and goodness of fit, Akaike's Information Criterion (AIC; Akaike, 1974), was calculated. AIC is defined as:

$$AIC = N \ln \sum_{i=1}^N (Y_i - \hat{Y}_i)^2 + 2 np \quad (1)$$

where N is the number of observations, Y_i is the observed value, \hat{Y}_i is the predicted value, and np is the number of parameters used to create the model. The preferred model is the one that has the smallest AIC. AIC acknowledges the goodness of fit of a model, but it also penalises the number of parameters used in the model. Thus, AIC discourages models that overfit the data. Both cross validation and AIC techniques have benefits and shortcomings in model selection (Arlot and Celisse, 2010).

3. Results and discussion

3.1. Characteristics of the infrared spectra on laboratory contaminated samples

The absorptions peaks in the mid-infrared spectral range were more pronounced compared to those in the near-infrared spectral range. The absorption peaks in MIR can be associated with known soil components and functional groups (Table 1).

The absorption peaks obtained from the portable MIR spectrometer and the laboratory benchtop MIR spectrometer were similar, as seen in Fig. 1 although the relative intensity of the peak might be different due to the different characteristics of the instruments. The absorption in the NIR region was due to the overtones of fundamental molecular vibration bands; thus, the absorption features were weak and undefined (Fig. 2).

3.1.1. Petroleum hydrocarbons peak characteristics

To be able to observe the effect of different variables clearly, known soil components were assigned to the specific wavelength region, as shown in Table 1. The absorption spectra in the MIR region for both

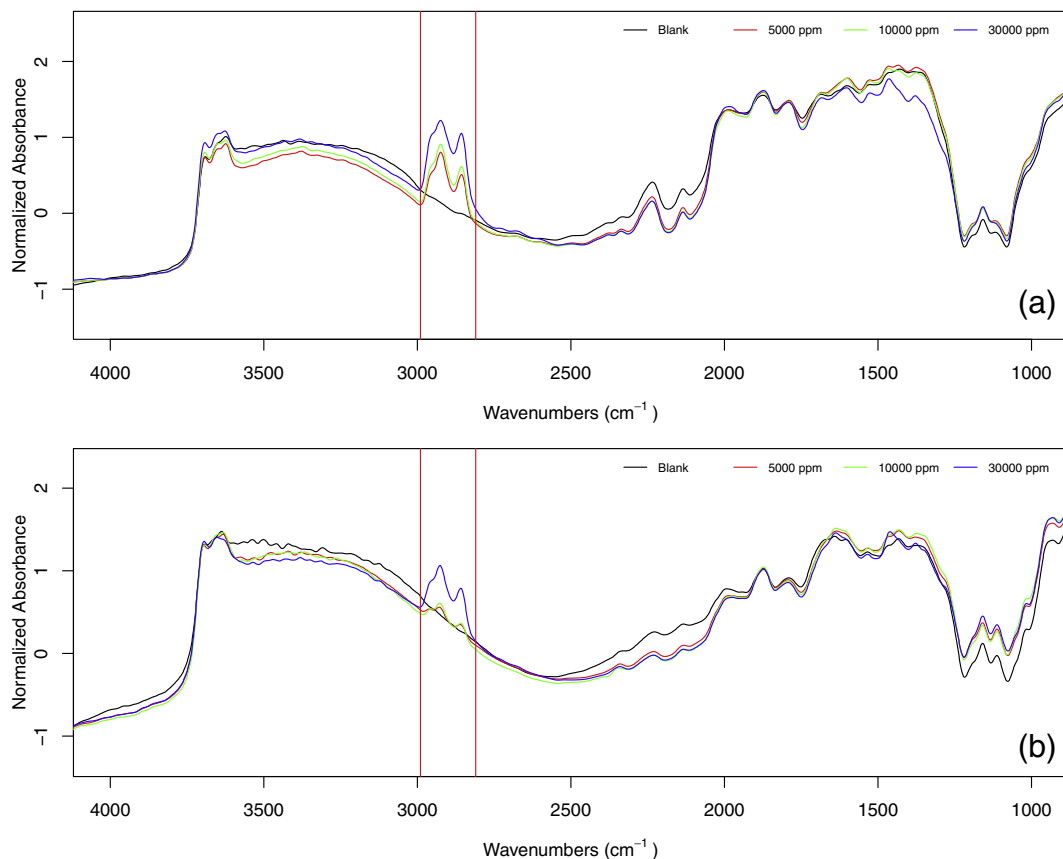


Fig. 3. Portable MIR spectra of (a) sandy and (b) clayey soil spiked with various concentrations of diesel. Peaks between 2990 and 2810 cm^{-1} were identified to be related to TRH concentration (aliphatic —CH₂, —CH₃).

sandy and clayey soil spiked with diesel at various concentrations can be seen in Fig. 3.

After the spectra were pre-processed, the background spectrum of soil was subtracted. From this, derived absorbance in the peaks around 2990–2810 cm^{-1} could be clearly observed. This peak was directly related to the concentration of the petroleum hydrocarbons applied to the soil. The higher the concentration of hydrocarbon contamination was, the higher the absorption peaks. Larger absorption of the motor oil contaminated soils is due to the larger amount of hydrocarbons in motor oil compared to those in diesel fuel.

Absorbance was more prominent in the sandy soil than clayey soil as seen in Figs. 1 and 3. This was due to the effect of the particle size on light scattering. Clayey soil, which has finer particles scatter more of the light; therefore, reducing the absorbance. A study conducted by Forrester et al. (2010) showed that porous clay minerals resulted in a weaker signal compared to non-porous sand. Clay minerals reflected more of the sorbed TPH spectra signal because it shielded the TPH within the soil structure.

For the NIR spectrophotometer, absorptions corresponded to the overtones and combinations of the fundamental bands. In the NIR spectra, the effect of hydrocarbon can be observed in the combination region around 2220 nm (Forrester et al., 2013; Chakraborty et al., 2015) and 2460 nm (Forrester et al., 2013), as well as the first overtone region around 1645 nm and 1752 nm, which is attributed to C—H stretching of ArCH, and C—H stretching of saturated CH₂ group (Chakraborty et al., 2015). This value is close to those reported by Okparanya and Mouazen (2013a) for hydrocarbon contaminated soil (1647, 1712 and 1759 nm). Because with increasing overtones, the absorption intensity decreased and band overlap increased, only the combination region

bands in 2300–2340 nm was analysed. An example of NIR spectra obtained in this study is shown in Fig. 3. Since soil texture is not active in the Vis-NIR region, the moisture was used as surrogate to relate the soil texture with clay content (Okparanya and Mouazen, 2013a). Due to the swelling characteristics of clay minerals, the higher the clay content, the higher the absorption peak is in the 950, 1450 and 1950 nm (Okparanya and Mouazen, 2013a). However, the addition of clay minerals decreases the TRH spectra signal in combination region.

3.1.2. The effect of organic matter

Remediation of petroleum-contaminated soil usually involves an addition of organic matter to enhance the breakdown of the hydrocarbons. The effect of organic carbon addition is minuscule in the 2990–2810 cm^{-1} region (the region related to the aliphatic groups/TRH concentration). However, it affected the region between 2100 and 1700 cm^{-1} (in particular the peaks at 1980, 1870, 1790 cm^{-1} region, seen in Fig. 4) which is attributed to the quartz overtone. To the best of our knowledge, the effect of decreasing absorbance in the quartz overtone region due to an increase in organic carbon content has not been analysed in other studies. However, this decrease is most likely due to the formation of mineral and organic carbon complexes in the soil. This complex has low sorption affinity for hydrocarbons, which might cause decrease absorption.

In the NIR region, visually, no specific peak on the absorption spectra can be seen to be affected by the organic matter. Thus, the first derivative of the absorption spectra was used to determine the affected wavelength (seen in Fig. 5), particularly in the 1400, 1900, and 2200–2400 nm region. From the derivative spectra, it can be deduced that addition of organic matter affected the region for hydroxides (1400,

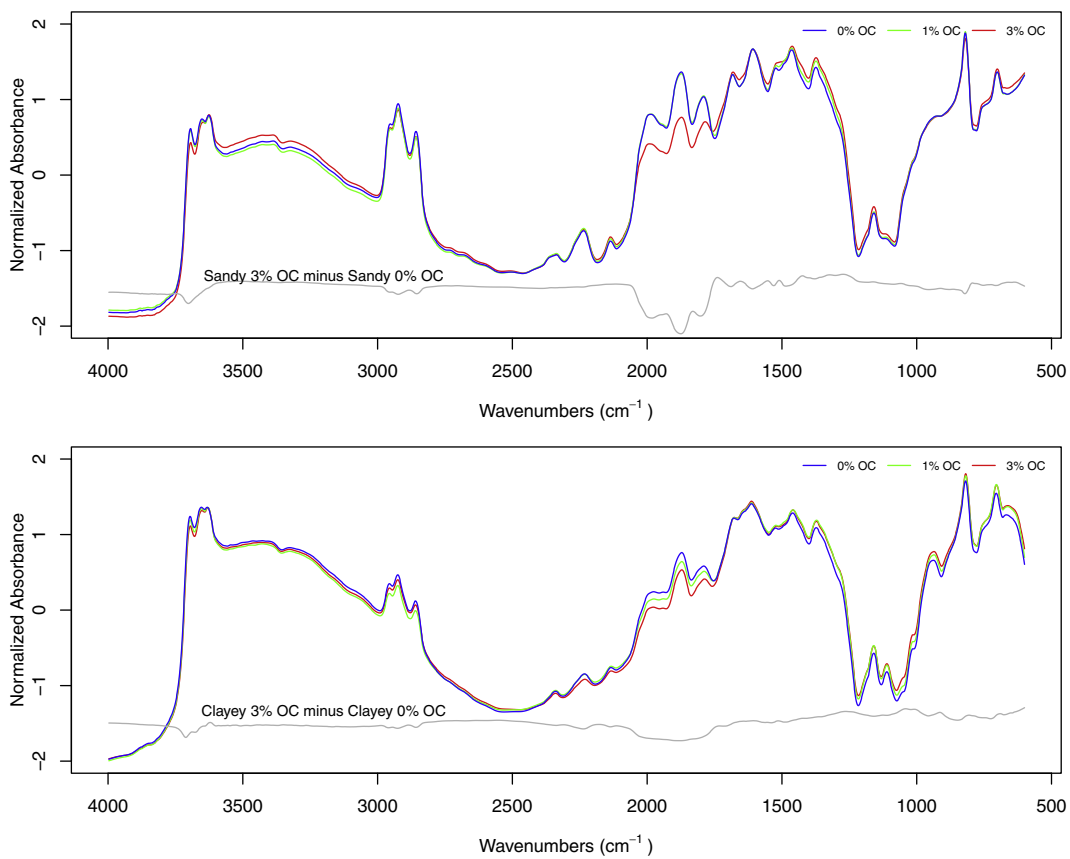


Fig. 4. Absorbance spectra in the MIR region of 30,000 ppm diesel contaminated (a) sandy and (b) clayey soil with various concentrations of added organic carbon.

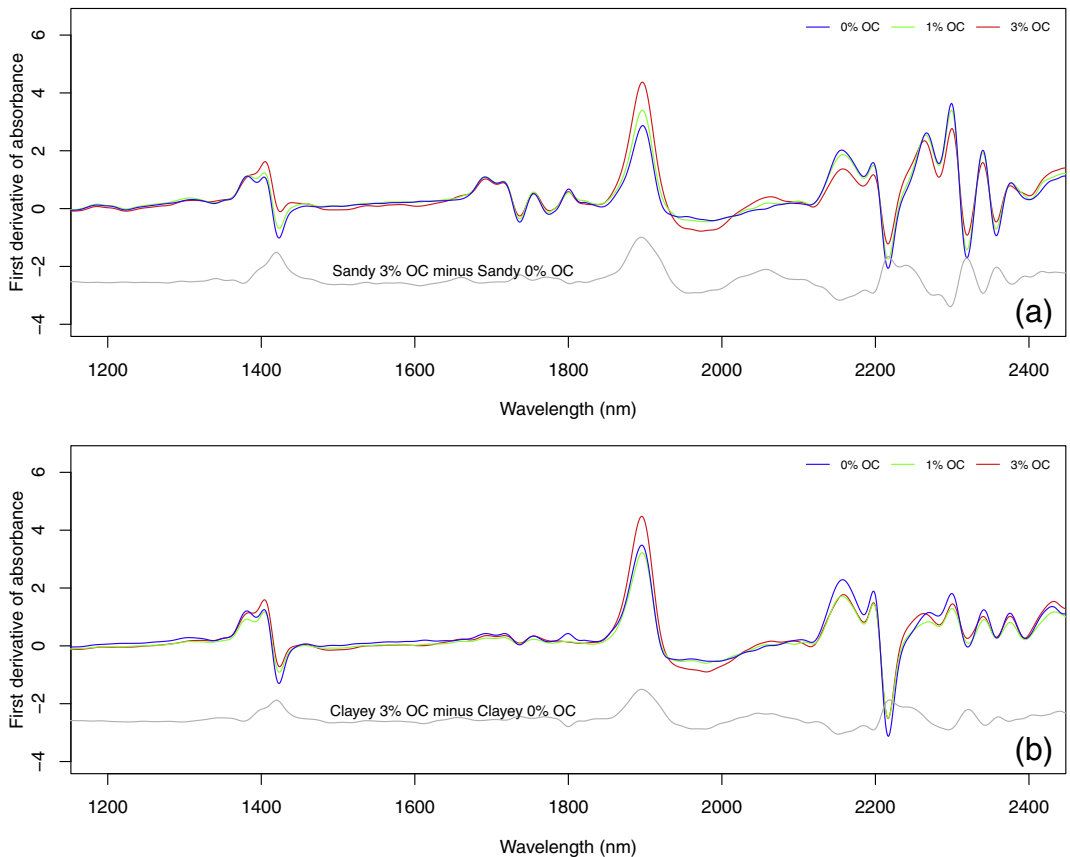


Fig. 5. First-derivative of absorbance spectra in the NIR region of 30,000 ppm diesel contaminated (a) sandy and (b) clayey soil with various concentrations of added organic carbon.

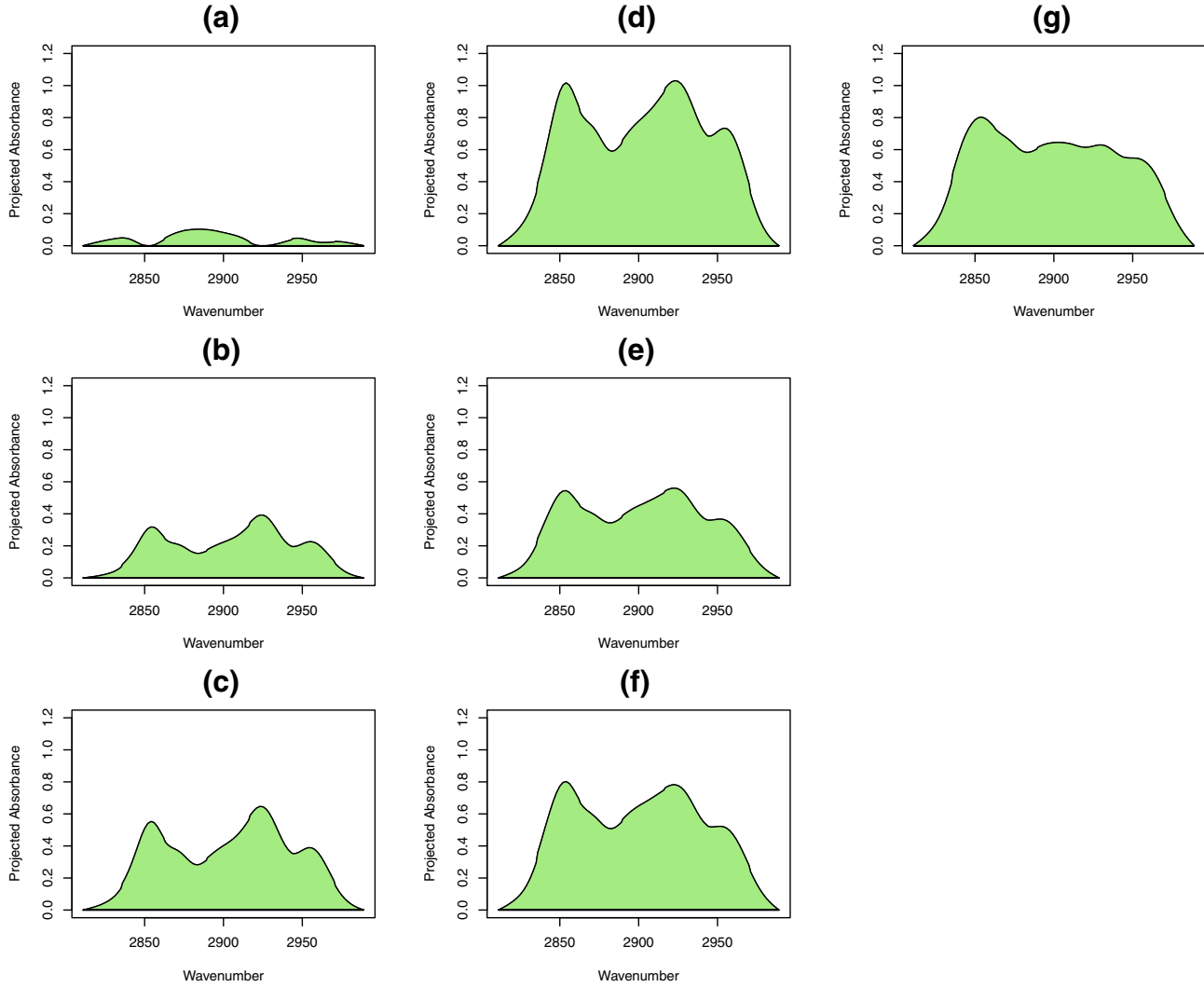


Fig. 6. Continuum-removed spectra between 2990 and 2810 cm^{-1} in the MIR region for sandy soils at (a) no addition (b) 5000 ppm diesel contamination, (c) 10,000 ppm diesel contamination, (d) 30,000 ppm diesel contamination, (e) 5000 ppm motor-oil contamination, (f) 10,000 ppm motor-oil contamination, (g) 30,000 ppm motor-oil contamination.

1900 nm) (Minasny et al., 2009; Okparanma and Mouazen, 2013a; Chakraborty et al., 2015) as well as the C—H stretching and bending region (~2200 nm) (Forrester et al., 2013).

3.1.3. Quantification of petroleum contamination using continuum-removed curve

To be able to compare the data in a more accurate manner, a continuum line was created by fitting a convex hull to the spectra within the specified wavelength bands. Comparisons of the area under the peaks of the continuum-line and continuum-removed spectra curve were used to compare one sample against the other, particularly in the region that is directly linked to hydrocarbon contamination. Comparisons of these continuum-removed areas for diesel fuel and motor oil contaminated sandy soils are shown in Fig. 6. Area quantification for different soil texture, organic carbon levels and contaminants using different infrared spectrometer are also shown in Figs. 7 and 8 (bars represent one standard deviation of the mean). The findings from the area quantification serve as a support for the findings claimed earlier in this paper. From the area quantification, the effect of soil texture can be clearly observed. Soil with clayey texture scatters more of the IR signal; therefore, it has less area compared to samples with sandy texture. Soils with a higher concentration of contaminant have a larger area compared to soils

with a lesser contaminant. Furthermore, soils contaminated with motor oil have larger area compared to those contaminated with diesel. This is expected due to longer carbon chain in motor oil. Also, the addition of organic matter content lowers the quantified area because of the formation of carbon complexes.

3.1.4. Petroleum hydrocarbons loss and degradation monitoring

The loss of hydrocarbons from the soil due to evaporation loss and degradation were analysed by taking measurements every 2–3 weeks for a total of 11 weeks observations, as seen in Figs. 9 and 10. Throughout time, the hydrocarbon loss in the samples was expected due to volatilisation. The effect of soil texture, organic matter content, types of contaminants and the concentrations on hydrocarbons loss using different spectrometers were compared.

Hydrocarbon loss occurred more rapidly in the sandy soil. The hydrocarbon seemed to be retained better in clayey soil in comparison to sandy soil. This is supported by the fact that minerals in the clayey soil might have formed complexes that prevent rapid loss in hydrocarbons, preventing rapid hydrocarbons loss. Addition of organic matter content created complex with the minerals, possibly inhibiting the hydrocarbon loss. Furthermore, motor oil is retained better within the soil compared to the diesel because it is less volatile.

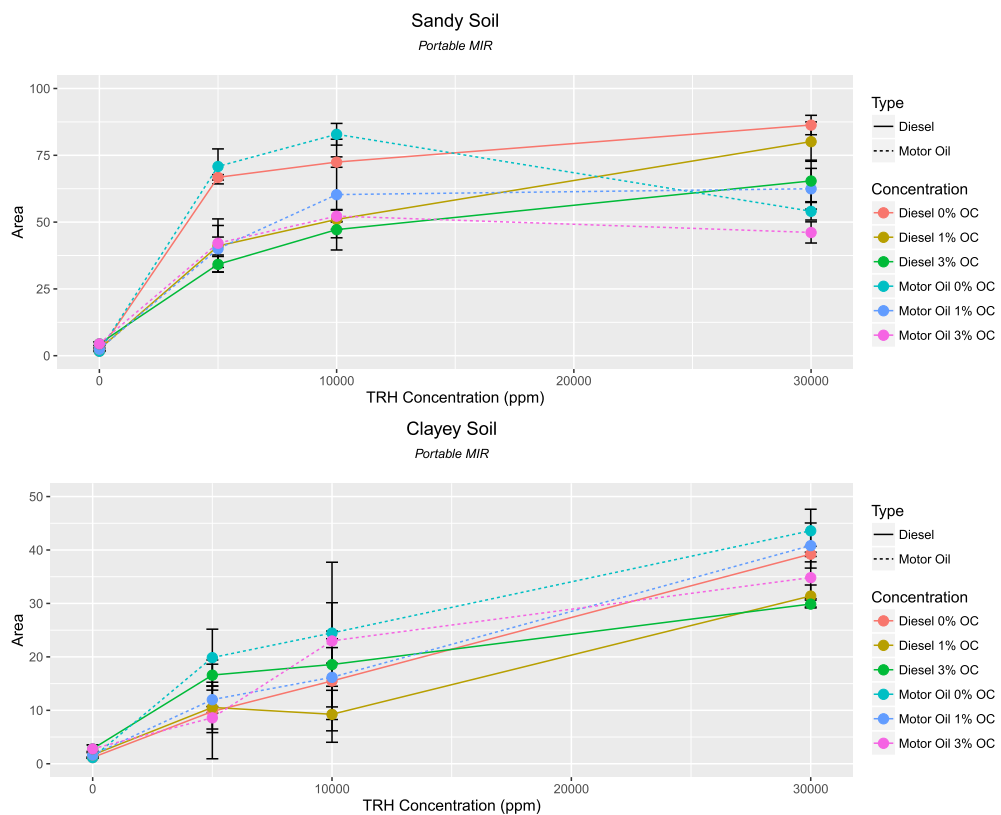


Fig. 7. Convex hull area between 2990 and 2810 cm^{-1} for sandy and clayey soils with different level of organic matter and different type of hydrocarbon contaminants at various concentrations using the portable MIR spectrometer. (Error bars represents $\pm 1\text{SD}$).

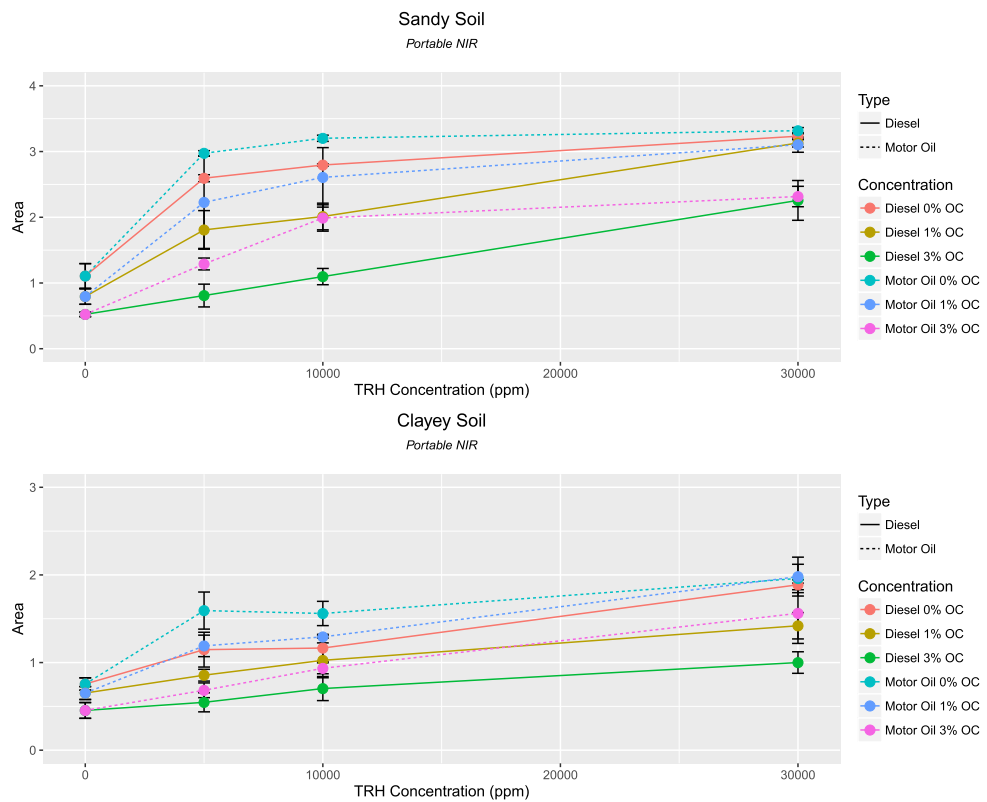


Fig. 8. Convex hull area between 2300 and 2340 nm for sandy and clayey soils with different level of organic matter and different type of hydrocarbon contaminants at various concentrations using portable vis-NIR spectrometers. (Error bars represents $\pm 1\text{SD}$).

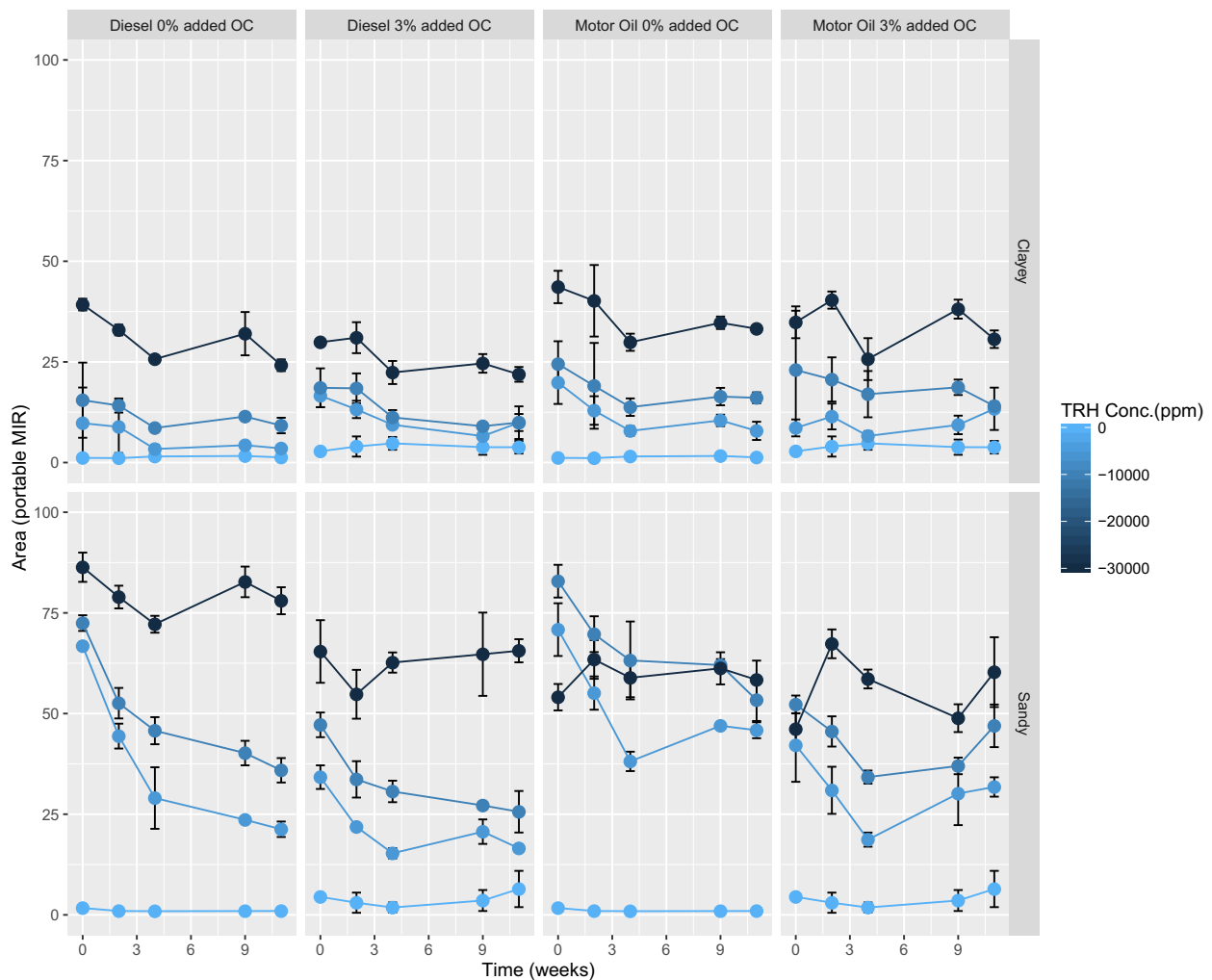


Fig. 9. Convex hull area between 2990 and 2810 cm^{-1} for sandy and clayey soils with different level of organic matter and different type of hydrocarbon contaminants at various concentrations throughout a period of 11 weeks. (see Supplementary materials for full comparison).

3.2. Validation of statistical models to predict TRH on field contaminated soils

Based on findings from laboratory-spiked samples, the regions affected by petroleum hydrocarbon were identified. Statistical models were then developed to predict the amount of TRH concentration in the actual field contaminated soils based on important wavelengths found in other published papers (Forrester et al., 2013; Hobley et al., 2014; Soriano-Disla et al., 2014).

We tested the method of “the area under specific peaks” calculated from the continuum-removed curve to quantify TRH concentration of field contaminated sites which had been analysed in the laboratory. The spectra collected from the field contaminated soils underwent the same pre-treatment processes as mentioned above (converted into absorbance, smoothed SG algorithm, then standardized with SNV transformations). The areas under the peaks from identified important wavelengths from the laboratory contaminated samples were used to test the accuracy of the model prediction.

Simple linear and multiple linear regression models were derived relating measured TRH with specific spectral areas from the NIR and MIR spectra. Table 2 shows the prediction accuracy using the three instruments. By using only the area under the peak between 2300 and 2340 nm in the NIR region, prediction of TRH using this linear model was poor. Similarly, the linear models that only use the area of region

2990–2810 cm^{-1} did not produce an accurate result for both portable and laboratory MIR spectrometers.

As the hydrocarbon peak can be affected by other soil organic components, we derived multiple linear regression models as follows:

$$\text{TRH}_{\text{portable MIR}} (\text{ppm}) = -1015 - 5500A + 1176B - 581C + 860D \quad (2)$$

$$\text{TRH}_{\text{laboratory MIR}} (\text{ppm}) = 2328 - 9739A + 1108B - 812C + 1061D \quad (3)$$

where A is the area under the peak between the region 1630–1580 cm^{-1} , B is the area between the region 1930–1840 cm^{-1} , C is the area between the region 2060–1930 cm^{-1} and D is the area between the region 2990–2810 cm^{-1} . The aromatic functional groups (1630–1580, 1930–1840, and 2060–1930 cm^{-1}) were found to be important predictors in addition to the more prominent aliphatic group 2990–2810 cm^{-1} . The specific spectra assignments for the bands were listed in Table 1. Although the model prediction improved, there were still large uncertainties of what other factors might affect the model.

In particular, the model based on the portable MIR performed better than the benchtop MIR instrument. Furthermore, the PLSR model calibrated on the portable MIR instrument (Eq. 2), ($\text{RMSE} = 2416 \text{ ppm}$) performed slightly better than the MLR model ($\text{RMSE} = 2577 \text{ ppm}$).

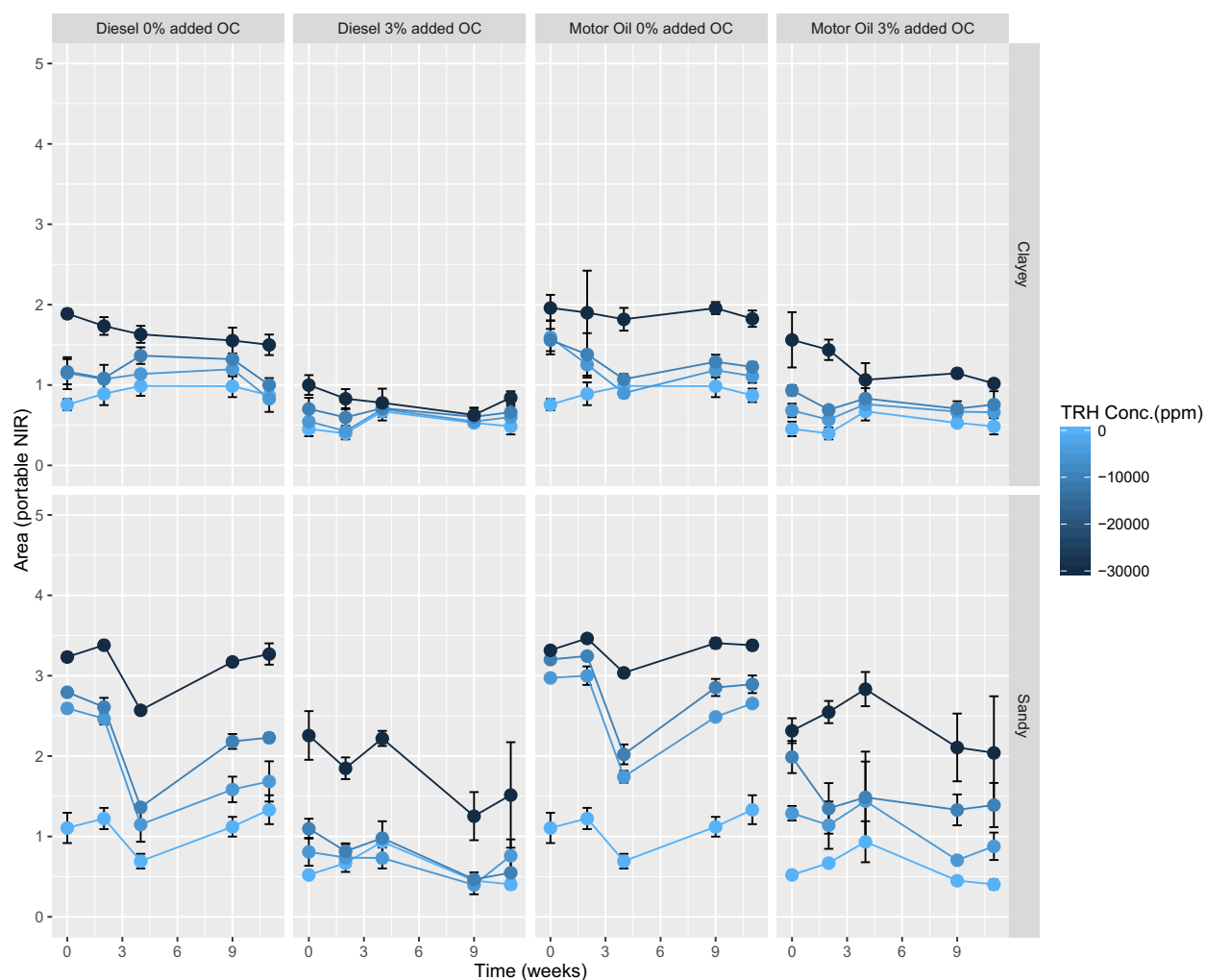


Fig. 10. Convex hull area between 2300 and 2340 nm for sandy and clayey soils with different level of organic matter and different type of hydrocarbon contaminants at various concentrations throughout a period of 11 weeks. (see Supplementary materials for full comparison).

Importantly, this error is lower than the Health Screening Level (HSL) for direct soil contact in residential areas of 18,500 ppm, and ESL of 3400–7540 ppm (NEPC, 2011a).

Here, the models are compared in terms of cross validated R^2 and RMSE, and also AIC values. In terms of cross validation, the PLSR models generally showed good prediction (Table 2). However, we are also

Table 2

Prediction of Total Recoverable Hydrocarbon (TRH) using spectra from different instruments and different number of predictors (np). LR is linear regression, MLR is multiple linear regression, PLSR is partial least squares regression, R² is coefficient of determination, RMSE is root mean squared error, and AIC is the Akaike Information Criterion calculated on calibration data (cal), and leave-one-out cross validation (cv).

Instrument	Predictors	np	R^2 cal	RMSE cal (ppm)	AIC cal	R^2 cv	RMSE cv (ppm)
Portable NIR	LR (2300–2340 nm)	2	0.25	4135	1511	0.17	4449
Portable NIR	PLSR (500–2450 nm)	196	0.84	1881	1786	0.58	3383
	N components = 9						
Portable MIR	LR 2990–2810 cm ⁻¹	2	0.57	3138	1477	0.54	3233
Portable MIR	MLR	5	0.75	2393	1438	0.71	2577
	1630–1580 cm ⁻¹						
	1930–1840 cm ⁻¹						
	2060–1930 cm ⁻¹						
	2990–2810 cm ⁻¹						
Portable MIR	PLSR (4000–650 cm ⁻¹)	180	0.89	1592	1730	0.75	2416
	N components = 8						
Laboratory MIR	LR	2	0.38	3754	1492	0.34	3862
	2990–2810 cm ⁻¹						
Laboratory MIR	MLR	5	0.59	3037	1457	0.53	3263
	1630–1580 cm ⁻¹						
	1930–1840 cm ⁻¹						
	2060–1930 cm ⁻¹						
	2990–2810 cm ⁻¹						
Laboratory MIR	PLSR (4000–650 cm ⁻¹)	177	0.89	1601	1724	0.77	2308
	N components = 9						

aware that the model maybe overfitting the data (Anderssen et al., 2006). Large numbers of parameters are used to create the PLSR model, compared with only 4 parameters used to create the MLR model. The PLSR coefficients for the portable and laboratory MIR (results presented in Supplementary materials) show different parts of the spectra as important predictors. More importantly, the PLSR models loadings and coefficients did not consider petroleum hydrocarbon peaks ($2990\text{--}2810\text{ cm}^{-1}$) as useful predictors. The PLSR models are able to fit the data better as they use a higher number of parameters as opposed to the linear model. It is notable that although the leave-one-out cross validation (cv) has higher RMSE values compared to calibration data (cal), the performance ranking for both cv and cal are the same (Table 2). Essentially cross validation provided the same information as calibration. Cross validation is known to provide an over-optimistic estimates of model performance and also can cause overfitting (Anderssen et al., 2006; Faber and Rajko, 2007; Esbensen and Geladi, 2010).

As an alternative, we evaluated the performance of the models taking into account their complexity or number of parameters. The results for laboratory MIR (Table 2) show that although the PLSR models produce the best fit in terms of R^2 and RMSE values, however the high number of parameters does not compensate for the improvement in RMSE values as calculated by AIC. The multiple linear models which use only 4 regions in the MIR consistently have lower AIC values, indicating that simpler models are preferred. This theoretical model quantification of TRH can be improved when more observations are collected.

4. Conclusions

This research explored methods for rapid detection of petroleum contamination in soils and demonstrated that infrared spectrometry can be utilized. In the laboratory experiment where soil samples were spiked with different concentrations of petroleum products, it was found that the portable mid-infrared spectrometer collected similar spectra as the laboratory benchtop mid-infrared spectrometer. Therefore, the portable MIR spectrometer could be used as a reliable soil sensor. The important infrared regions to quantify hydrocarbon contamination are near $2990\text{--}2810\text{ cm}^{-1}$ (MIR), and $2300\text{--}2340\text{ nm}$ (NIR). The clay and carbon contents were found to decrease the TRH spectra signal. The laboratory contaminated soil study showed that throughout the study period of 11 weeks, hydrocarbon losses due to volatilisation and degradation were negligible compared to other factors, such as soil texture, organic carbon content and types of contaminants.

Based on the laboratory results, attempts were made to predict petroleum hydrocarbon concentration on field contaminated soils from NIR and MIR spectra. It was found that TRH can be predicted with a multiple linear model developed using only 4 regions in the MIR spectra ($R^2_{\text{portable MIR}} = 0.71$; $R^2_{\text{lab MIR}} = 0.53$). There is an indication that commonly-used PLSR models potentially overfit the data by utilizing a large numbers of parameters. Therefore, future development of models based on infrared spectra should consider the fundamental bands as predictors. Although more datasets are needed to build a more robust model, an initial estimation of petroleum contamination can be obtained from this multiple linear regression model approach. Further work will look into the predictability of different carbon fractions of the TRH.

Acknowledgements

The authors acknowledge Environmental Earth Sciences for providing the field contaminated samples. This work is part of an ARC Linkage Project LP150100566 - Optimised field delineation of contaminated soils.

Appendix A. Supplementary data

Supplementary data to this article can be found online at <http://dx.doi.org/10.1016/j.geoderma.2016.11.030>.

References

- Akaike, H., 1974. A new look at the statistical model identification. *IEEE Trans. Autom. Control* 19, 716–723.
- Anderssen, E., Dyrstad, K., Westad, F., Martens, H., 2006. Reducing over-optimism in variable selection by cross-model validation. *Chemom. Intell. Lab. Syst.* 84 (1–2), 69–74.
- Arlot, S., Celisse, A., 2010. A Survey of Cross-validation Procedures for Model Selection. pp. 40–79.
- Chakraborty, S., Weindorf, D.C., Li, B., Aldabaa, A.A.A., Ghosh, R.K., Paul, S., Ali, M.N., 2015. Development of a hybrid proximal sensing method for rapid identification of petroleum contaminated soils. *Sci. Total Environ.* 514, 399–408.
- Clark, R.N., 1999. Spectroscopy of rocks and minerals, and principles of spectroscopy. *Remote sensing for the earth science. Manual of Remote Sensing*, third ed. vol. 3. John Wiley and Sons, New York.
- Clark, R.N., Roush, T.L., 1984. Reflectance spectroscopy: quantitative analysis techniques for remote-sensing applications. *J. Geophys. Res.* 89 (B7), 6329–6340.
- CRCCARE (Cooperative Research Centre for Contamination Assessment and Remediation of the Environment), 2015s. Annual Report 2014–2015. Cooperative Research Centre for Contamination Assessment and Remediation of the Environment, Newcastle, Australia. (Available at:). http://www.crcare.com/files/dmfile/CRCCARE_AnnualReport_2014-15.pdf.
- Esbensen, K.H., Geladi, P., 2010. Principles of proper validation: use and abuse of re-sampling for validation. *J. Chemom.* 24 (3–4), 168–187.
- Faber, N.M., Rajko, R., 2007. How to avoid over-fitting in multivariate calibration – the conventional validation approach and an alternative. *Anal. Chim. Acta* 595 (1–2), 98–106.
- Forrester, S.T., Janik, L., McLaughlin, M., 2010. An Infrared Spectroscopic Test for Total Petroleum Hydrocarbon (TPH) Contamination in Soils. Proceedings of the 19th World Congress of Soil Science, Soil Solutions for a Changing World, Brisbane, Australia.
- Forrester, S.T., Janik, L.J., McLaughlin, M.J., Soriano-Disla, J.M., Stewart, R., Dearman, B., 2013. Total petroleum hydrocarbon concentration prediction in soils using diffuse reflectance infrared spectroscopy. *Soil Sci. Soc. Am. J.* 77 (2), 450–460.
- Hastie, T., Tibshirani, R., Friedman, J., 2009. *The Elements of Statistical Learning*. second ed. Springer Series in StatisticsSpringer-Verlag, New York (Data mining, inference, and prediction).
- Hobley, E., Willgoose, G.R., Frisia, S., Jacobsen, G., 2014. Vertical distribution of charcoal in a sandy soil: evidence from DRIFT spectra and field emission scanning electron microscopy. *Eur. J. Soil Sci.* 65 (5), 751–762.
- Horta, A., Malone, B., Stockmann, U., Minasny, B., Bishop, T.F.A., McBratney, A.B., Pallasser, R., Pozza, L., 2015. Potential of integrated field spectroscopy and spatial analysis for enhanced assessment of soil contamination: a prospective review. *Geoderma* 241, 180–209.
- Minasny, B., McBratney, A.B., Pichon, L., Sun, W., Short, M.G., 2009. Evaluating near infrared spectroscopy for field prediction of soil properties. *Aust. J. Soil Res.* 47 (7), 664–673.
- NEPC (National Environment Protection Council), 2011a. Schedule B1 - Guideline on Investigation Levels for Soil and Groundwater. National Environment Protection (Assessment of Site Contamination) Measure (NEPM), Canberra, Australia (Standing Council on Environment and Water. Available at: <http://www.scew.gov.au/system/files/resources/93ae0e77-e697-e494-656f-afaa9fb4277/files/schedule-b1-guideline-investigation-levels-soil-and-groundwater-sep10.pdf>).
- NEPC (National Environment Protection Council), 2011b. Schedule B3 - Guideline on Laboratory Analysis of Potentially Contaminated Soils, National Environment Protection (Assessment of Site Contamination) Measure (NEPM), Canberra, Australia (Standing Council on Environment and Water. Available at: <http://www.scew.gov.au/system/files/resources/93ae0e77-e697-e494-656f-afaa9fb4277/files/schedule-b3-guideline-laboratory-analysis-potentially-contaminated-soils-sep10.pdf>).
- Okparama, R.N., Mouazen, A.M., 2013a. Visible and near-infrared spectroscopy analysis of a polycyclic aromatic hydrocarbon in soils. *Sci. World J.* vol. 2013, 160360 (9 pages, 2013).
- Okparama, R.N., Mouazen, A.M., 2013b. Determination of total petroleum hydrocarbon (TPH) and polycyclic aromatic hydrocarbon (PAH) in soils: a review of spectroscopic and nonspectroscopic techniques. *Appl. Spectrosc. Rev.* 48 (6), 458–486.
- R Core Team, 2016. R: A Language and Environment for Statistical Computing. R Foundation for Statistical Computing, Vienna, Austria Available at: <https://www.R-project.org/>.
- Rinnan, A., van den Berg, F., Engelsen, S.B., 2009. Review of the most common pre-processing techniques for near-infrared spectra. *TrAC Trends Anal. Chem.* 28 (10), 1201–1222.
- Sadler, R., Connell, D., 2003. Analytical Methods for the Determination of Total Petroleum Hydrocarbons in Soil. Proceedings of the 5th National Workshop on the Assessment of Site Contamination, May 2003NEPC Serv. Corp., Adelaide, SA, Australia.
- Schwartz, G., Ben-Dor, E., Eshel, G., 2012. Quantitative analysis of total petroleum hydrocarbons in soils: comparison between reflectance spectroscopy and solvent extraction by 3 certified laboratories. *Appl. Environ. Soil Sci.*
- Soriano-Disla, J.M., Janik, L.J., Rosse, R.A.V., Macdonald, L.M., McLaughlin, M.J., 2014. The performance of visible, near-, and mid-infrared reflectance spectroscopy for prediction of soil physical, chemical, and biological properties. *Appl. Spectrosc. Rev.* 49 (2), 139–186.
- Viscarra Rossel, R.A., Adamchuk, V.I., Sudduth, K.A., McKenzie, N.J., Lobsey, C., 2011. Proximal soil sensing: an effective approach for soil measurements in space and time. *Adv. Agron.* 113, 237–282.
- Viscarra Rossel, R.A., Raphael, A., McBratney, A.B., Minasny, B., 2010. Proximal soil sensing. *Progress in soil science*Springer, Dordrecht; New York.